JOURNAL OF SOLID STATE CHEMISTRY **123,** 60–67 (1996)
ARTICLE NO. 0152

Short and Medium Range Order in Ga–Ge–S Glasses: An X-Ray Absorption Spectroscopy Study at Room and Low Temperatures

A. M. Loireau-Lozac'h,*[,1] F. Keller-Besrest,† and S. Bénazeth‡[,]§

*Laboratoire de Chimie Physique Générale et Minérale, Faculté de Pharmacie, Université Paris V, 4 Ave de l'Observatoire, F 75270 Paris, France; †Laboratoire de Physique et Biomathématiques, Faculté de Pharmacie, Université Paris V, 4 Ave de l'Observatoire, F 75270 Paris, France; ‡Laboratoire LURE, Université Paris-Sud, F 91405 Orsay, France; §Laboratoire de Chimie Physique Minérale et Bioinorganique, Faculté de Pharmacie, Université Paris-Sud, F 92296, Chatenay-Malabry, France

Received July 20, 1995; in revised form January 17, 1996; accepted January 23, 1996

Glasses belonging to the Ga_2S_3–GeS_2 line are studied at room temperature and at 7 K by XAFS spectroscopy at Ga and Ge K-edges. The results show that the addition of Ga_2S_3 to the GeS_2 glass former leads to the formation of tetrahedral units of GaS_4, linked to the GeS_4 tetrahedra. Mainly low temperature measurements of the Ge K-edge allow an analysis of the short and medium range order. As the Ga content increases a substitution takes place of corner-sharing linkages with edge-sharing linkages of $(Ge/Ga)S_4$ tetrahedral units.

1. INTRODUCTION

Besides the semiconducting chalcogenide glasses based on former elements such as germanium or arsenic, there exists a wide class of chalcogenide gallium based glasses which are less often described. These glasses present peculiar behavior since it is impossible to obtain bulk Ga–S or Ga–Se binary glasses by using conventional quenching. The glassy state is therefore reached by synthesis of more complex materials which contain either modifier elements (such as rare earth elements) or some former elements (such as germanium) (1–3). These materials then display thermal and physical properties which can be used in micro- or photoelectronics (4, 5). Furthermore, they are used as hosts for rare-earth doped glasses which are important in fiber-amplifier and mid-infrared laser applications (6). Some structural studies of these glasses have been developed (3), but they did not explain why there are no binary sulfide or selenide gallium glasses, and leave open the question of the low glass forming ability of gallium. To answer some of these questions, we studied mixed gallium and germanium sulfide glasses in order to compare local and medium range order (if they exist) around the gallium and germanium atoms. We chose to work with the quasi-binary system Ga_2S_3–GeS_2 for which a glass forming domain extends from GeS_2 to the composition with $n = 0.55$ (n = Ga/(Ga + Ge)). The XAFS spectroscopy (X-ray absorption fine structure) is well suited to investigate separately the evolution of Ga and Ge short range order surroundings as a function of cation ratios. When performed at low temperature (LT), this technique allows us to attempt medium range order information. Two different XAFS studies were done: one of the Ga K-edge, and the other of the Ge K-edge.

2. EXPERIMENTAL AND METHOD

All the bulk samples have been prepared from Ga_2S_3–GeS_2 sulfides mixed with the desired stoichiometry. The mixtures were melted in silica ampoules at 1373 K and then quenched with cold water. X-ray diffraction diagrams were registered to verify the glassy state. Three glassy compositions were prepared: (1) and (3) are close to the boundaries of the glass-forming region, while (2), with $n = 0.30$, has an intermediate composition.

sample (1)	9 GeS_2–0.5 Ga_2S_3	($n = 0.10$)
sample (2)	7 GeS_2–1.5 Ga_2S_3	($n = 0.30$)
sample (3)	3 GeS_2–1 Ga_2S_3	($n = 0.40$)

As references we used compounds $La_6Ga_2Mn_2S_{14}$ (7) and αGeS_2 (8) in which the Ga or Ge sulfur surroundings are quasi-tetrahedral.

To acquire the XAFS data, the samples and reference compounds were ground to powder, with a grain size less than 20 μm. X-ray absorption spectroscopy measurements were carried out on the XAFS II station at the DCI storage ring of LURE (Orsay) at the Ga (10367 eV) and Ge (11104 eV) K-edges. Transmission mode measurements were done at room temperature and at 7 K using a helium liquid cryostat. Energy selection was made using a Si (311) double crystal monochromator. Considering the relatively high

[1] To whom all correspondence should be addressed.

0022-4596/96 $18.00

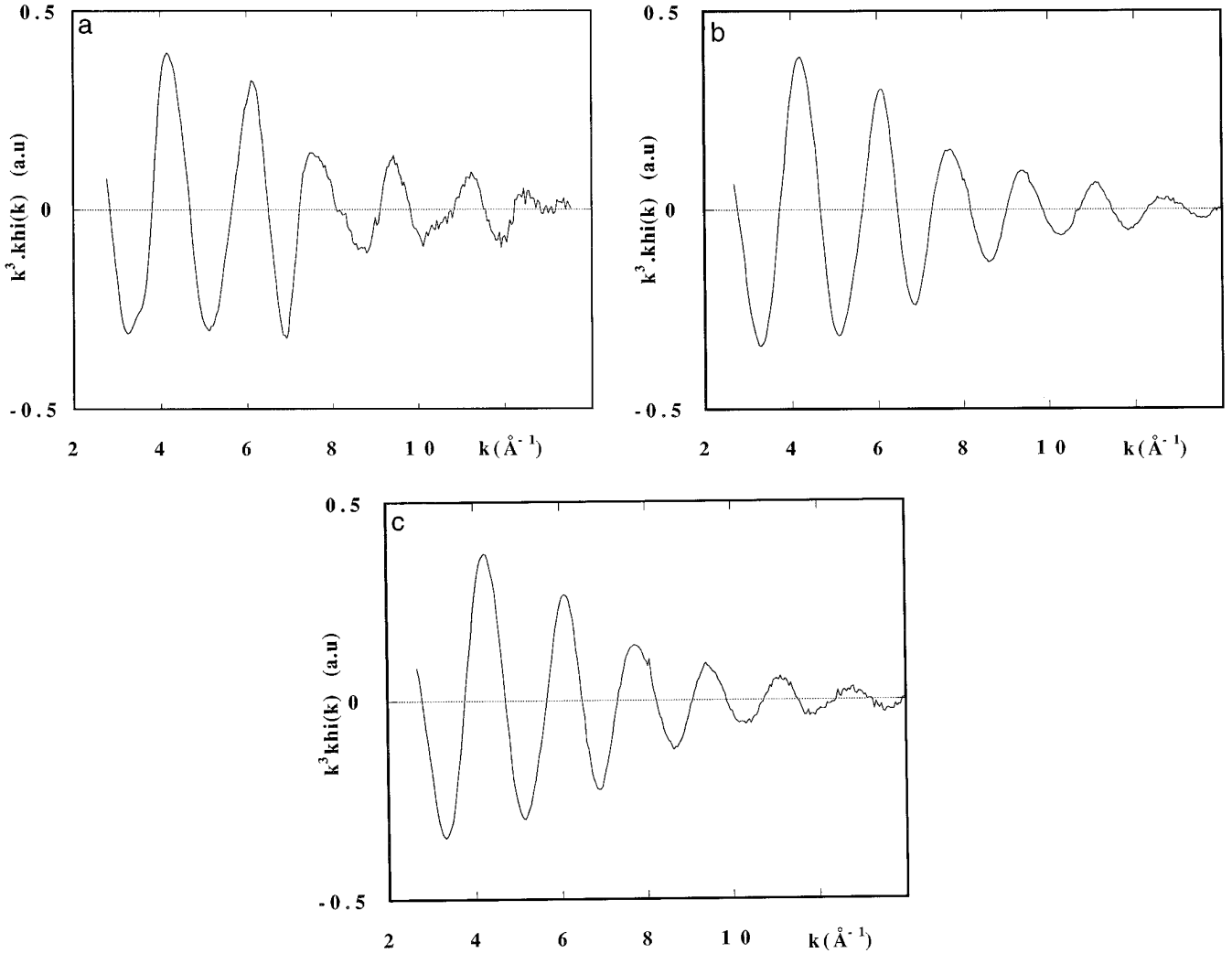

FIG. 1. Normalized XAFS oscillations extracted at germanium K-edge and 7 K for (a) αGeS_2, (b) sample 1, and (c) sample 3.

energy of the K-edges studied no rejection harmonic mirrors were used.

We tried to collect data at the S K-edge (2472 eV) in transmission mode, but in the glassy matrix, the high Ge and Ga atom content (these atoms have a high atomic number with respect to the sulfur element) induces the absorption of the S K-edge excitation photons. Therefore, obtained measurements could not be analyzed, but collecting a new set of data in fluorescence mode will avoid this problem.

The XAFS analytical procedure in the single scattering theory and the in-plane-wave approximation has been fully described elsewhere (9). For the data analysis we used the program package from A. Michalowicz, ''EXAFS pour le Mac'' (10). The spectra of the three samples and the reference compounds have been analyzed following the same procedure: the normalized XAFS function (Fig. 1a, 1b, 1c) is obtained from the Lengeler–Eisenberger formula (11), with a linear model for the pre-edge background removal, and the post-edge absorption being reproduced by a third degree polynomial function. For each of the compounds studied, the E_0 edge energy is taken at the inflection point. A first filtering in the k space conserves wave vector k values between 2.6 and 11.3 $Å^{-1}$ for the Ga K-edge spectra, and between 2.8 and 13 $Å^{-1}$ for the Ge K-edge spectra. Low frequency oscillations are removed by using selection criteria to keep R greater than 1.1 and 1.30 Å, respectively, in the first pseudo-radial distribution functions (pseudo-RDF) around the Ga and Ge atoms. After a back Fourier transform to the k space, the filtered XAFS signals are k^3 weigthed and Fourier transformed through a Kaiser window ($\tau = 2$) in the range from about 4 to 12 $Å^{-1}$.

During the fitting procedure, we used theoretical phases and amplitude functions from McKale *et al.* (12). In this

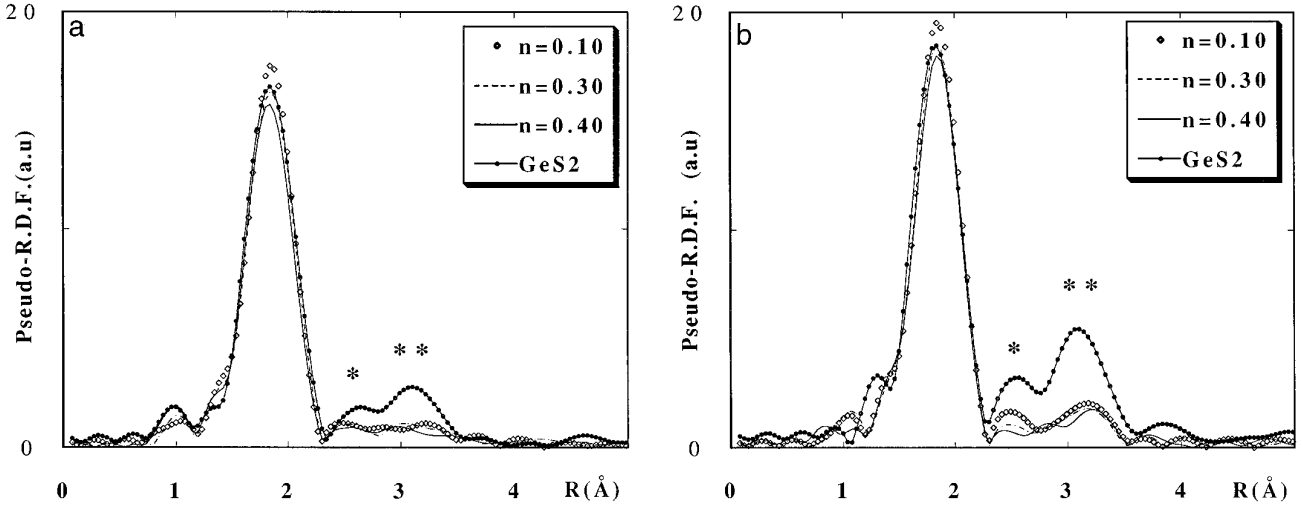

FIG. 2. Pseudo-radial distribution function around the Ge atoms (a) at RT and (b) at 7 K. (*) Short Ge–Ge distance (2.92 Å), (**) long Ge–Ge distance (3.41 Å).

case it is necessary to determine the correction term ΔE_0 of the absorption edge threshold relative to the different atomic pairs considered, cation–sulfur and cation–cation, and to the Γ parameter related to the mean free path of the photoelectron in the considered compounds. These parameters, which will be used later again in the two sets of the refinement procedures of low and room temperature measurements, are obtained from the modelization based on structural data and from characteristical peaks of the reference compounds, also registered at these two temperatures.

All the Fourier transforms presented here are uncorrected from phase shift, and so the R distances appearing in the pseudo-radial distribution functions have to be increased to nearly 0.4 Å.

The main peak from the αGeS_2 pseudo-RDF of the reference compound (Fig. 2a or 2b), filtered according to the criterion $1.15 < R < 2.30$ Å, corresponds to a quasi-regular tetrahedron of GeS_4 with R(Ge–S) = 2.22 Å. The modelization of its spectrum allows the refinement of six independent parameters. The crystallographic data are introduced, and the ΔE_0 term for the atomic pair Ge–S is first refined, and successively the parameter Γ, and the Debye–Waller factor σ is related to the thermal and structural disorder.

The second and third peaks of the αGeS_2 pseudo-RDF correspond to the surrounding of the germanium atoms with two shells of germanium atoms at different distances R(Ge–Ge) = 2.92 and 3.40 Å. This double peak is filtered ($2.3 < R < 3.5$ Å) allowing the refinement of six independent parameters, and its XAFS spectra is modeled according to the previous double shells described from crystallographic data. The two shells are described with common ΔE_0 and Γ values. The refined values are then used for further analysis of the Ge–Ge atomic pairs in the samples.

In order to model the gallium surroundings, Ga_2S_3 is not used as a reference compound, as it presents many crystallographic sites and dispersed Ga–S distances. Among numerous crystalline compounds, $La_6Ga_2Mn_2S_{14}$ (7) was the best for comparison with the glasses, because it showed a more regular gallium coordination (three Ga–S distances at 2.28 Å, and one at 2.23 Å, so an averaged Ga–S distance = 2.27 Å). The manganese cation did not disturb the XAFS analysis at the Ga K-edge performed on this reference compound. The previous procedure evoked for the determination of ΔE_0 and Γ parameters concerning the study at the Ge K-edge is applied to the treatment of the pseudo-RDF main peak from the $La_6Ga_2Mn_2S_{14}$ reference compound (filtering criterion: $1.0 < R < 2.4$ Å). Its modelization (seven independent parameters) gives the ΔE_0 correction term for the Ga–S atomic pair and the Γ parameter for the XAFS analysis at the Ga K-edge.

The XAFS analytical procedure previously described for the reference compounds is applied to the glassy samples. During the fitting procedures, first, the ΔE_0 parameter related to the atomic pair studied is allowed to vary slightly. Afterward, the number of scattering atoms in the concerned shell (N value) and its average distance R from the central atom considered are refined. In the final refinement cycles, the N, R, ΔE_0, and σ parameters were allowed to vary, but the Γ value was kept fixed.

During the fitting procedures numerous assays were performed with different initial parameters whose values were allowed to vary. Most converged to convenient structural

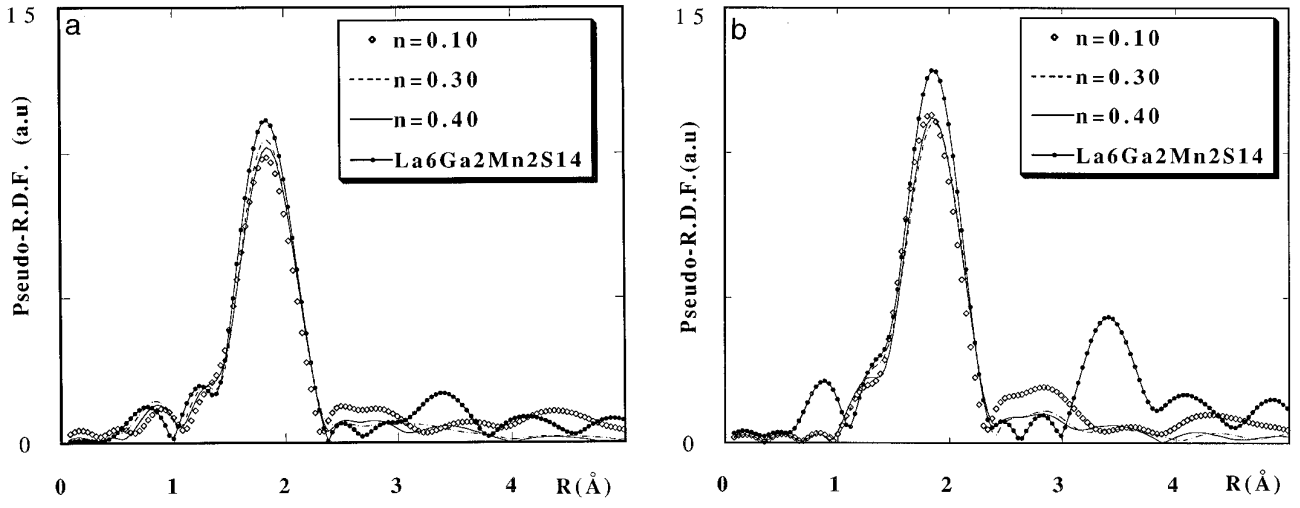

FIG. 3. Pseudo-radial distribution function around the Ga atoms (a) at RT and (b) at 7 K.

parameters with a coherent evolution versus the composition. For each of the studied compounds, four spectra were recorded and independently refined in order to evaluate the resulting precision. The final N, R, and σ values are the average of these four refinements, and the error was deduced from their dispersion.

3. RESULTS

3.1. Ga K-Edge

Figures 3a and 3b present the pseudo-radial distribution functions (Fourier transform of $k^3\chi(k)$) around the Ga K-edge for the reference compound and the three glassy samples, at room (RT) and low temperatures, respectively (see also Table 1 and 2).

The main peak corresponds to the Ga–S shell. For the three glassy samples, the peak intensity is independent of the Ga composition. This is confirmed by the N fit values very close to four, which also confirms the tetrahedral GaS_4 coordination.

On the LT pseudo-RDF figure (Fig. 3b), where the peaks are well isolated, one sees on the pseudo-RDF reference compound a double peak at about R = 3.4 Å. This is attributed to the gallium second shell composed of sulfur and lanthane atoms, as deduced from the structural data of this crystalline compound (7). It is strongly enhanced when compared to the room temperature spectra (Fig. 3a). This feature shows the importance of LT measurements to reveal higher shells. Medium range order around Ga atoms cannot be easily identified on the entire glassy sample pseudo-RDF series. However, for the vitreous sample with n = 0.10, a week broad peak appears with a maximum at 2.8 Å, which should correspond to a shell distance at about 3.2 Å after the phase correction. It is attributed to Ga–Ga or Ga–Ge distances. The atomic configuration of Ga and Ge atoms just differs by one electron, and these atoms have similar atomic radii. These characteristics limit our XAFS analysis discrimination between these two atoms. We exclude a Ga–Ga interaction, since the peak intensity decreases with the Ga content (from n = 0.1 to 0.4). This assumption is based on a homogeneous picture of the glassy structure. However, it does not exclude the

TABLE 1
Fit Results Concerning the S Shell around Ga Atoms, in Ga_2S_3–GeS_2 Glasses at Room Temperature

	$n = \frac{Ga}{Ga+Ge}$	N	R (Å)	σ (Å)[a]	ΔE_o (eV)	RF[b] ($\times 10^{-2}$)
$La_6Ga_2Mn_2S_{14}$		4	2.28(2)	0.09	6.0	1.3
Sample 1	0.10	4.1(4)	2.28(2)	0.10	6.2	1.8
Sample 2	0.30	4.1(4)	2.28(2)	0.09	6.3	1.4
Sample 3	0.40	4.1(4)	2.28(2)	0.10	5.8	1.7

[a] The error term is less than 0.01 Å.
[b] RF: reliability factor.

TABLE 2
Fit Results Concerning the S Shell around Ga Atoms, in Ga_2S_3–GeS_2 Glasses at Low Temperature (7 K)

	$n = \frac{Ga}{Ga + Ge}$	N	R (Å)	σ (Å)[a]	ΔE_o (eV)	RF[b] ($\times 10^{-2}$)
$La_6Ga_2Mn_2S_{14}$		4	2.28(2)	0.08	6.45	1.1
Sample 1	0.10	4.0(4)	2.28(2)	0.09	6.37	0.8
Sample 2	0.30	4.0(4)	2.28(2)	0.09	6.03	0.9
Sample 3	0.40	4.1(4)	2.28(2)	0.09	6.42	0.9

[a] The error term is less than 0.01 Å.
[b] RF: reliability factor.

existence of Ga_2S_3 clusters for low Ga contents, but this XAFS analysis cannot evidence them. We propose to attribute this peak to a Ga–Ge distance, as a similar peak appears in the pseudo-RDF of the same sample studied around the Ge atoms (Fig. 2b). In this figure, the medium range order around Ge atoms is well evidenced: it is mainly due to short and long Ge–Ge distances, and may also contain a contribution of Ge–Ga atomic pairs. This hypothesis of some Ge atoms surrounding Ga atoms in the second shell, with a Ga–Ge distance on the order of 3.2 Å, is supported by the fact that the intensity of the corresponding peak in the pseudo-RDF around the Ga atoms decreases with the Ge content in the glassy samples.

It can be concluded from this study at the Ga K-edge, that the Ga atoms are engaged in GaS_4 tetrahedra, and in Ge rich glassy samples Ga–Ge interactions are proposed with distances on the order of 3.2 Å.

3.2. Ge K-Edge

Figures 2a and 2b present the pseudo-RDF functions obtained around Ge atoms, at RT and LT, for the αGeS_2 reference compound and the glassy samples. The main peak corresponds to the first shell of sulfur atoms. The fit results obtained from each sample are presented in Tables 3 and 4. Both are quite similar, except the decreasing σ values at low temperature. The N and R values for the different samples are always close to the corresponding parameters in the αGeS_2 reference compound. This shows that the tetrahedral surrounding of S atoms around Ge atoms is insensitive to the Ga content, except that the GeS_4 tetrahedra distortion increases slightly with the Ga content.

The main interest of the low temperature measurements is to reveal a second shell around Ge atoms which permits us to approach medium range order informations. Figure 2b clearly shows on the pseudo-RDF second and third peaks in the range from 2.3 to 3.5 Å. This feature is well defined for the reference compound αGeS_2. Its magnitude decreases as the Ga content increases in the glassy sample. The crystalline αGeS_2 structure (Fig. 4) is known to have a layered structure built up from chains of GeS_4 corner-sharing tetrahedra. These chains, which are noted "a" in Fig. 4, are themselves connected through links of two GeS_4 edge-sharing tetrahedra, which are noted "b." The second coordination sphere of Ge atoms is therefore made up of a short Ge–Ge distance (2.92 Å) related to edge-sharing tetrahedra, while a long Ge–Ge distance (3.41 Å) corresponds to the corner-sharing tetrahedra, which form the third Ge coordination shell. (This structural feature has been analyzed by XAFS (13) relatively to the binary Ge–S glasses.)

We chose to analyze independently the main peak corresponding to the sulfur shell, and the weak double peak extending from 2.3 to 3.5 Å, because (as seen in Fig. 2b),

TABLE 3
Fit Results Concerning the S Shell around Ge Atoms, in Ga_2S_3–GeS_2 Glasses at Room Temperature

	$n = \frac{Ga}{Ga + Ge}$	N_1	R (Å)	σ (Å)[a]	ΔE_o (eV)	RF[b] ($\times 10^{-2}$)
αGeS_2		4	2.22(2)	0.07	8.0	2.8
Sample 1	0.10	4.0(4)	2.23(2)	0.07	7.8	1.9
Sample 2	0.30	3.9(4)	2.22(2)	0.08	8.6	1.3
Sample 3	0.40	3.9(4)	2.22(2)	0.08	7.8	1.7

[a] The error term is less than 0.01 Å.
[b] RF: reliability factor.

TABLE 4
Fit Results Concerning the S Shell around Ge Atoms, in Ga_2S_3–GeS_2 Glasses at Low Temperature (7 K)

	$n = \frac{Ga}{Ga + Ge}$	N_1	R (Å)	σ (Å)[a]	ΔE_o (eV)	RF[b] ($\times 10^{-2}$)
αGeS_2		4	2.22(2)	0.06	7.1	2.5
Sample 1	0.10	4.0(4)	2.23(2)	0.07	6.7	2.2
Sample 2	0.30	4.0(4)	2.22(2)	0.07	7.5	1.9
Sample 3	0.40	4.1(4)	2.22(2)	0.07	7.5	1.5

[a] The error term is less than 0.01 Å.
[b] RF: reliability factor.

these two kinds of peaks are always well resolved independently from the Fourier transform conditions applied.

Based on the filtering of the double peak, the fit of the model of a Ge–Ge double shell is performed on the reference compound αGeS_2. A set of fits, with close reliability factor values but some differences in the structural parameters obtained, are performed on each of the glassy samples. We rejected those which could not correspond to a structural interpretation. (During the fitting procedures, the two shells are described with common ΔE_0 and Γ parameter values.)

Figures 5a, 5b, and 5c present the $k^3 \cdot \chi(k)$ curve fits for αGeS_2, for the glassy samples 1 with $n = 0.10$ and 2 with $n = 0.30$.

In Table 5 are summarized the fit results of the second and third Ge shells at low temperature for αGeS_2 and the three glassy samples. Keeping in mind that XAFS analysis cannot discriminate between Ge or Ga backscattering atoms, these results describe the short and long Ge–(Ge/Ga) distances characteristic of edge- and corner-sharing tetrahedral units, respectively.

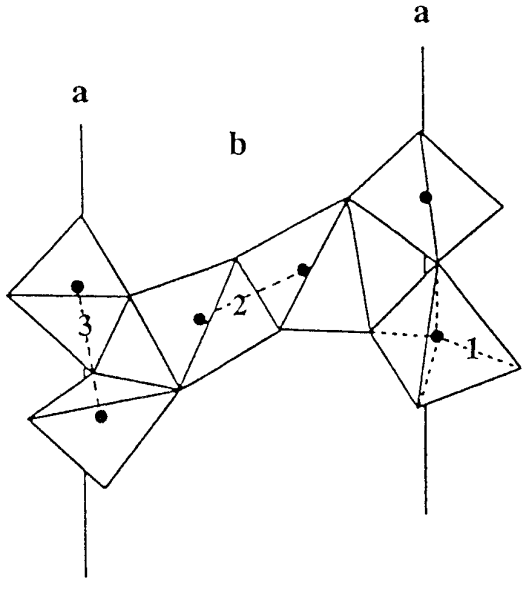

FIG. 4. Structure of αGeS_2. (1) Ge–S distance, (2) short Ge–Ge interaction, (3) long Ge–Ge interaction.

Our previous results from the Ga K-edge studies have shown that the addition of Ga gives rise to GaS_4 tetrahedral units with Ga–S distances significantly higher (2.28 Å) than the Ge–S distances (2.22 Å) in GeS_4 tetrahedral units. The Ga insertion in the structural organization may maintain the global αGeS_2 structure, but distorting it through edge- or corner-sharing linkage of GaS_4 tetrahedra substituted for GeS_4 units. However, the addition of Ga_2S_3 to GeS_2 (Ge_2S_4) results in a defect of sulfur atoms, which prevents the maintenance of the αGeS_2-type tetrahedral units linkage. This sulfur defect implies a compensation by the formation of edge linkages between $(Ge/Ga)S_4$ tetrahedral units. This idea of the disappearance of some corner linkages with respect to the αGeS_2 structural organization involves a decrease in the number N_3 of the long Ge–(Ge,Ga) distances as the Ga content increases. This is clearly observed in Table 5. The introduction of larger GaS_4 units into the Ge atoms' surrounding shell creates an important distortion in the surrounding figure. This is translated by the high σ values obtained for this shell when compared to the corresponding σ value obtained for αGeS_2. As the Ga content increases in the glassy samples, the number N_2 of the short Ge–(Ge,Ga) interactions between edge-sharing tetrahedral units also decreases. Indeed, the substitution of corner linkages by edge linkages between mixed $(Ge/Ga)S_4$ tetrahedral units of different sizes and positions around the shared edge involve Ge–(Ge,Ga) distances which are intermediate between the short and long ones, characteristic of the two types of linkage in αGeS_2. These intermediate distances are not evidenced here, possibly because of their wide dispersion, especially for lower Ga content. However, one can see in Fig. 2b that the second and third peaks related to the short and long Ge–(Ge,Ga) distances analyzed here evolve to a figure made of three weak peaks for the higher Ga content ($n = 0.40$) glassy sample. We tried to fit this third

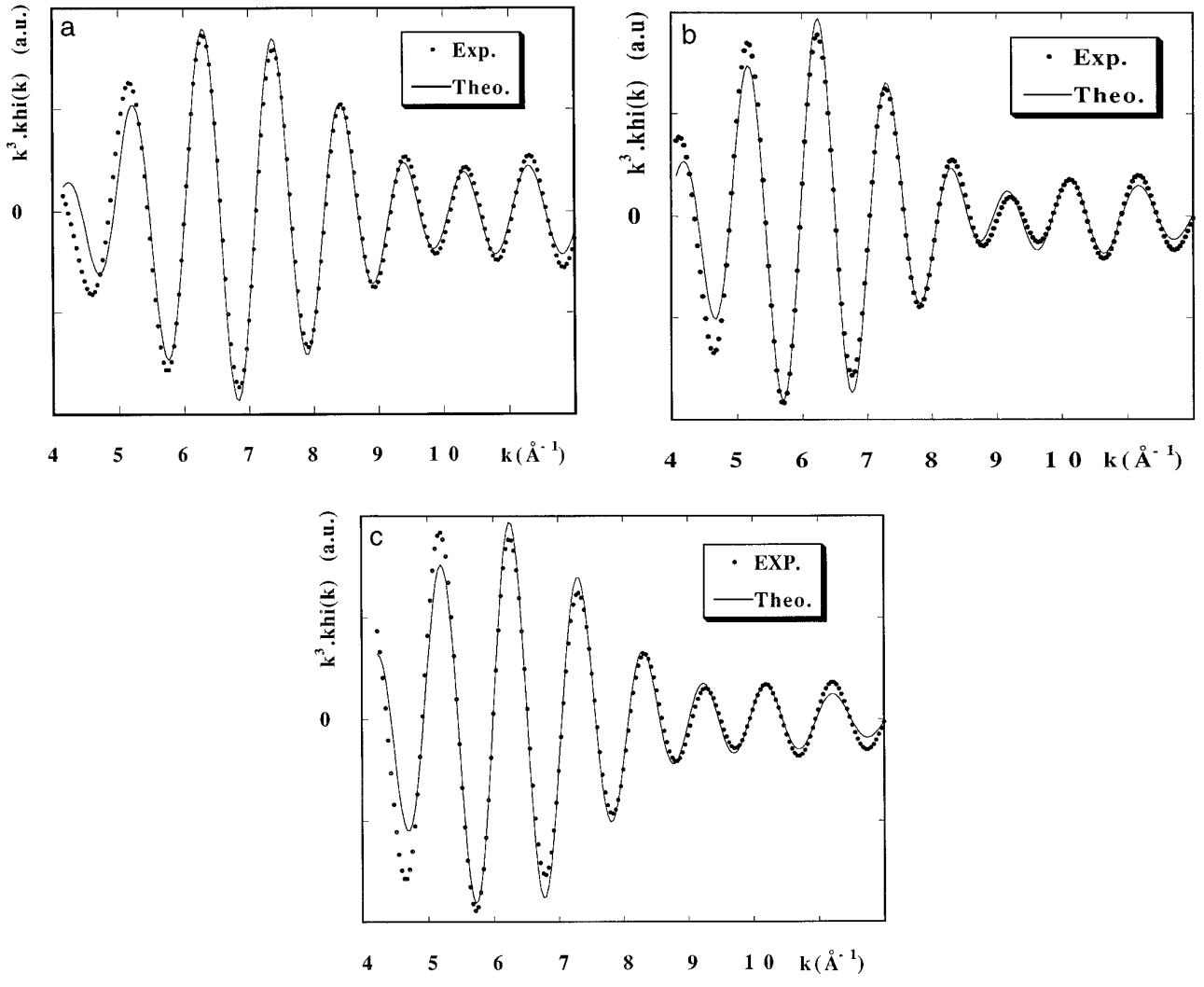

FIG. 5. $k^3 \cdot \chi(k)$ curve fit of the double peak corresponding to the short and long Ge–Ge distances in (a) αGeS_2, (b) sample 1, and (c) sample 2.

peak by introducing in the model a shell corresponding to an approximate distance Ge–(Ge,Ga) of 3.2 Å. Unfortunately, taking into account the error bar, the number of these interactions obtained was not significant. However, the existence of such intermediate Ge–Ga distances on the order of 3.2 Å has been suggested previously during the discussion about the LT Ga K-edge results. As observed in Table 5, the $N_2 + N_3$ value decreases from 3.4 to 2.8 when the Ga content increases, which is explained here by the loss of these intermediate Ge–(Ge/Ga) distances. The

TABLE 5
Fit Results Concerning the Short and Long Ge–(Ge/Ga) Distances in Ga_2S_3–GeS_2 Glasses, at the Ge K-Edge and Low Temperature (7 K)

	$n = \frac{Ga}{Ga + Ge}$	N_2	R_2 (Å)	σ (Å)[a]	N_3	R_3 (Å)	σ (Å)[a]	RF[b] ($\times 10^{-2}$)
αGeS_2		1	2.92(2)	0.08	3	3.41(2)	0.07	
Sample 1	0.10	0.6(1)	2.90(2)	0.09	2.8(3)	3.44(2)	0.11	2.4
Sample 2	0.30	0.5(1)	2.90(2)	0.10	2.4(2)	3.43(2)	0.11	4.1
Sample 3	0.40	0.3(1)	2.90(2)	0.09	2.5(2)	3.43(2)	0.12	3.2

[a] The error term is less than 0.01 Å.
[b] RF: reliability factor.

$KGaGeS_4$ crystalline structure (14) presents, in respect to the metal atom Ga and Ge organization, a great similarity with the αGeS_2 structure. But here, these metal atoms are statistically distributed between the center of corner- or edge-sharing $(Ge/Ga)S_4$ tetrahedral units, and one recovers a distribution of the metal distances between a short one (2.97 Å) and three long ones (from 3.47 to 3.53 Å) associated to the tetrahedra linkage type. This evidences the possibility of two types of connections between mixed tetrahedral units, and confirms that the glassy structural organization involves the breaking of the long range order between chains and pairs of $(Ge/Ga)S_4$ tetrahedra.

4. DISCUSSION

This XAFS analysis clearly establishes the formation of GaS_4 tetrahedra, but with very weak medium range order interactions. These are attributed to widely distributed Ga–Ge interactions, which support a weak signal in the XAFS spectra. In contrast, a clustering mechanism of the GaS_4 tetrahedra which should involve Ga–Ga interactions can be excluded.

In the glassy matrix, the mechanism consists of replacing some GeS_4 tetrahedra by GaS_4, but due to the defect of sulfur which results in the addition of Ga_2S_3 to GeS_2, the αGeS_2 structural organization is highly modified by the formation of edge linkage in place of corner linkage between the tetrahedral units.

This structural model of the Ga–Ge–S glasses studied here is built of GaS_4 and GeS_4 tetrahedra, both edge- and corner-sharing, supporting different Ga–S or Ge–S average distances. We don't have evidence for a clustering tendency of the GaS_4 units, even for the richest Ga glassy composition. Such an organization where the Ga atoms are quite dispersed in the Ge–S glassy matrix could not be reached by an exclusively binary Ga–S composition. However, it would be helpful to complete this work by scattering techniques to describe the medium range order.

Our results are not in agreement with the models proposed by Ivanova (4) concerning the $(GeS_2)_{100-x}Ga_x$ glasses studied by vibrational spectroscopy, neutron scattering, and X-ray diffraction. These models do not respect GaS_4 tetrahedra which are well described by our XAFS measurements and do not propose mixed edge- and corner-sharing GeS_4 and GaS_4 tetrahedra.

Moreover, our results bring structural information which may be applied to the Ga–Ge–Se system, studied by Giridhar and Mahadevan (15), where sulfur is replaced by selenium: in such glasses the gallium atoms probably present a four coordination and do not obey to the 8-*N* rule as we have observed in the Ga–Ge–S system investigated here.

REFERENCES

1. A. M. Loireau-Lozac'h, Thèse d'Etat, Paris, 1977.
2. F. Auzel, J. C. Michel, J. Flahaut, A. M. Loireau-Lozac'h, and M. Guittard, *C. R. Acad. Sci. Paris* **291,** 21 (1980).
3. S. Bénazeth, M. H. Tuilier, A. M. Loireau-Lozac'h, H. Dexpert, P. Lagarde, and J. Flahaut, *J. Non-Cryst. Solids* **110,** 89 (1989).
4. Z. G. Ivanova, *J. Mol. Struct.* **245,** 335 (1991).
5. N. Chbani, X. Cai, A. M. Loireau-Lozac'h, and M. Guittard, *Mater. Res. Bull.* **27,** 1355 (1992).
6. K. Wei, D. P. Machewirth, J. Wenzel, E. Snitzer, and G. H. Sigel, Jr., *Opt. Lett.* **19,** 904 (1994).
7. N. Rodier, M. Guittard, and J. Flahault *C. R. Acad. Sci. Paris* **296,** 65 (1983).
8. G. Dittmar and H. Schäfer *Acta Crystallogr. B* **31,** 2060 (1975).
9. B. K. Teo, "Basic Principles and Data Analysis." Springer Verlag, New York, 1986.
10. A. Michalowicz, XAFS pour le Mac, *in* "Logiciels pour la Chimie" p. 102. Société Française de Chimie, Paris, 1991.
11. B. Lengeler and P. Eisenberger, *Phys. Rev. B* **21,** 4507 (1980).
12. A. G. McKale, B. W. Veal, A. P. Paulikas, S. K. Chan, and S. Knapp, *J. Am. Chem. Soc.* **110,** 3763 (1988).
13. P. Armand, A. Ibanez, H. Dexpert, and E. Philippot, *J. Non-Cryst. Solids* **139,** 137 (1992).
14. P. Wu, Y. J. Lu, and J. A. Ibers, *J. Solid State Chem.* **97,** 383 (1992).
15. A. Giridhar and S. Mahadevan, *J. Non-Cryst. Solids* **126,** 161 (1990).